

# An Exploration of Multivariate Fluctuation Dissipation Operators and Their Response to Sea Surface Temperature Perturbations

DAVID FUCHS, STEVEN SHERWOOD, AND DANIEL HERNANDEZ

*Climate Change Research Centre, University of New South Wales, Sydney, New South Wales, Australia*

(Manuscript received 26 March 2014, in final form 27 July 2014)

## ABSTRACT

The fluctuation–dissipation theorem (FDT) has been proposed as a method of calculating the mean response of the atmosphere to small external perturbations. This paper explores the application of the theory under time and space constraints that approximate realistic conditions. To date, most applications of the theory in the climate context used univariate, low-dimensional-state representations of the climate system and an arbitrarily long sample size.

The authors explore high-dimensional multivariate FDT operators and the lower bounds of sample size needed to construct skillful operators. It is shown that the skill of the operator depends on the selection of variables and features representing the climate system and that these features change once memory (slab ocean) is added to the system.

In addition, it is found that the FDT operator has skill in estimating the response to realistic sea surface temperature (SST) patterns, such as El Niño–Southern Oscillation (ENSO), despite the fact that these patterns were not part of the data used to produce the operator. The response of clouds is also studied; for variables that represent cloud properties, the decrease in skill in relation to decrease in sample size still maintains the key features of the response.

## 1. Introduction

Leith (1975) proposed the use of the fluctuation–dissipation theorem (FDT) as a method for determining atmospheric response to external perturbations. At its core, the theory yields an operator that estimates the mean response of a system from observations of unforced fluctuations. Such an operator can then be used in sensitivity studies. For example, when only the mean response is desired, an FD operator can replace an ensemble of more expensive model integrations (Gritsun and Branstator 2007, hereafter GB07; Gritsun et al. 2008, hereafter GBM08). A more general purpose in applying the theory is to test the conceptual and practical limits of our understanding of climate.

Since Leith's proposal, several alternative derivations of the theory in the climate context have been proposed for time-invariant cases (Bell 1980; Gritsoun et al. 2002; Majda et al. 2005, 2010), time-periodic cases (Majda and

Wang 2010), and nonparametric time-invariant cases (Cooper and Haynes 2011). To date, however, tests of the theory on a full atmosphere-like global climate model (GCM) consisted mostly of the basic form of the theory [Gritsun (2010) being an exception]. In this form, the unperturbed atmosphere is assumed to follow a time-invariant probability density function (PDF) and this PDF is assumed to be sufficiently close to Gaussian [or quasi Gaussian as was coined in Majda et al. (2005)]. An application of FDT to determine steady-state response of the climate system generally comes with an additional assumption that the climate system is ergodic in its nature. As a consequence, the averaged response of an ensemble of simulations can be replaced with the time average of a sufficiently long single trajectory. This is an attractive property if the theory is to be applied on direct observations. With all these assumptions in place, the operator boils down to an integration of lag covariances and an inverse covariance.

Let the unperturbed atmosphere be accessed through the state vector  $\mathbf{x}$ . Given a small but constant external perturbation  $\delta f$ , the mean deviation (response) from the unperturbed climate mean  $\langle \delta \mathbf{x} \rangle$  is estimated through Eq. (1):

---

*Corresponding author address:* David Fuchs, Climate Change Research Centre, University of New South Wales, Level 4, Mathews Building, Sydney NSW 2052, Australia.  
E-mail: d.fuchs@unsw.edu.au

$$\langle \delta \mathbf{x} \rangle = \int_0^{N_\tau} \mathbf{C}(\tau) \mathbf{C}(0)^{-1} d\tau \delta f, \quad (1)$$

where the angle brackets denote a time mean,  $\mathbf{C}(\tau) = \langle \mathbf{x}(\tau) \mathbf{x}(0)^T \rangle$  is the lag- $\tau$  covariance matrix, and  $\mathbf{C}(0)^{-1}$  denotes the inverse of the lag-zero covariance matrix. It is assumed that long-term means were removed from the state vector before calculating the covariances. Since we are interested in the estimate of steady state response, the upper bound of the integral should, in principle, be infinite. In practice, the integral is bounded by the sample size of the data; hence,  $N_\tau$  is finite but sufficiently large to capture the time scale of a response.

A second form of the operator correlates the perturbation of the state  $\mathbf{x}$  to some known function of the state  $\mathbf{A}(\mathbf{x})$  (Majda et al. 2005; Risken 1984). In this case, Eq. (1) generalizes to

$$\langle \delta \mathbf{A}(\mathbf{x}) \rangle = \int_0^{N_\tau} \mathbf{C}_A(\tau) \mathbf{C}(0)^{-1} d\tau \delta f, \quad (2)$$

where  $\mathbf{C}_A(\tau)$  denotes the lag- $\tau$  covariance matrix  $\langle \mathbf{A}[\mathbf{x}(\tau)] \mathbf{x}(0)^T \rangle$ . GBM08 took this idea a step further and assumed the existence of a functional relation between a climate variable and the state of the operator.

When the quasi-Gaussian assumption is made, the response operator is nothing more than a sum of linear-regression operators. Such a result may be considered an oversimplification considering the scale and complexity of the climate system. What is then the justification for such an approach? The literature shows a mix of successes and failures in applying the theory to the climate system. Kirk-Davidoff (2009) shows that a univariate low-dimensional operator fails to show skill given a limited sample size in a system that is forced through stochastic perturbation. Similarly, Ring and Plumb (2008) show a significant nonlinear response in a GCM to axisymmetric forcing. Their experiments show that an approach that follows similar derivation as Eq. (1) fails to approximate the response of the annular modes to this kind of forcing. In contrast, GB07 and GBM08 show that the same equation has high skill in estimating the response to local perturbations in a simple atmosphere only GCM.

Inspection of these and other experiments reveals significant differences between these studies, especially in assumptions that go beyond the theory and relate to application to climate. First, there are significant differences in the way the climate state is described. While most studies use a low-dimensional operator, GB07 and GBM08 attempt to capture as many dimensions as possible from the full phase space of a GCM. It is argued that the high dimensionality of the operator is needed in order to sample the chaotic attractors of the climate

system [for more on this topic, refer to Gritsoun et al. (2002), Majda et al. (2005), and references therein]. A second reason to capture as many dimensions as possible concerns the model reduction approach and will be discussed in the next section. Another aspect of the dimensionality of the operator is the number of climate variables used. Most studies (GB07 being an exception) consider the climate state as being captured by a single quantity—commonly, temperature. This, however, may not be sufficient since it may only sample part of the chaotic attractors that compose the climate system. GB07, in contrast, used an operator composed from two variables—one dynamic and the other thermodynamic.

The second point of divergence is the differences in the sample size used to construct the operator. These range from 5 to 12 000 years of data with some additional variability in sampling rates. Sample size is related to the dimensionality of the operator (and the climate system in general) since the amount of spatial dimensions required in order to construct a robust operator poses a hard lower bound on the amount of data required. For example, adding more variables to the operator may add skill but it may also increase the lower bound of the data if the problem is to remain well posed. While the general assumption is that the sample size is large enough not to pose a problem, the scarcity of climate data drives the applications of the theory using arbitrary amount of data (e.g., Cionni et al. 2004). In principle, one hopes to find a minimal set of variables that forms a robust operator for a given system and external perturbation.

Another source of errors, related to the chaotic nature of the climate system, is the finding that the Gaussian approximation produces the wrong results when the external forcing is applied along the stable direction of the attractor (Colangeli and Lucarini 2014). This observation motivated the development of alternative algorithms that combine the information contained in the observable instead of the PDF. For example, Abramov and Majda (2007) “blends” the short-term prediction made on the observable with the long-term prediction made by a stable algorithm such as the Gaussian approximation. Their approach depends on the ability to identify a tangent model of the observable and a “blending” point, from which the stable algorithm takes over. Recent theoretical advances seem to follow this path (Baiesi and Maes 2013; Colangeli and Lucarini 2014). Baiesi and Maes (2013) provides a unified view of approaches that operate on the observable and those that operate on the PDF. At the same time, Colangeli et al. (2012) argue that the construction of an operator from a projection, or a subset, of the phase space offers some benefits in mitigating the deficiencies described above. However, in order to focus on issues relating to dimensionality and sample size, the

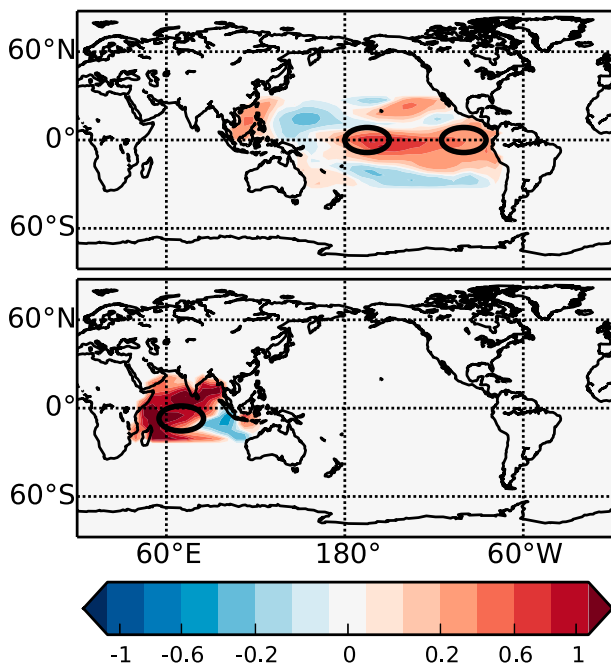


FIG. 1. SST perturbation patterns used. The ellipses represent the location of Gaussian patterns and the colored patches represent the (top) ENSO-like pattern and (bottom) positive IOD-like pattern.

operators used in this work rely on the presence of an invariant PDF along with the Gaussian approximation to that PDF.

Finally, although FDT applies as an approximation of the atmosphere, it is important to consider the relation to the surface. Much of the atmospheric response can be attributed to the interaction with surface patterns such as ENSO. From the perspective of FDT, changes to these patterns can be considered as an external perturbation.

The following sections are organized as follows. [Section 2](#) describes the experimental setup, the construction of the FD operator, and the model reduction approach that was used. The relation between skill to dimensionality, sample size, and memory are then explored in [section 3](#). We conclude with a discussion in [section 4](#).

## 2. Methodology

### a. Experimental setup

To study the response operator under different scenarios, we work with a GCM of intermediate complexity—namely, Mk3L ([Phipps 2010](#)). The atmospheric component of Mk3L uses a R21 truncation, which amounts to 18 hybrid vertical levels and  $64 \times 56$  grid points on the horizontal, offering a balance between complexity and performance. It is also integrated with a land surface model and may be augmented with ocean or slab components.

TABLE 1. Definition of forcing patterns.

Pattern (ID)	Location	Type
Central western Pacific (CWP)	0°, 165°W	Gaussian
Eastern Pacific (EP)	0°, 100°W	Gaussian
Indian Ocean (IO)	7°S, 70°E	Gaussian
ENSO	25°N–25°S, Pacific	Realistic ( <a href="#">Santoso et al. 2012</a> )
Positive IOD	Indian Ocean	Gaussian

Even in these relatively coarse settings, it is impractical to use a climate variable (i.e., temperature  $T$ ) in its unreduced form in an operator (as was done in [GB07](#) and [GBM08](#); more on that in [section 2b](#)). To compare the results to [GB07](#) and [GBM08](#), the GCM is fixed to a single-season boundary condition. This also conforms with the assumption that the PDF of the system is stationary.

Two model configurations are used to produce the data, from which response operators are created: first, a fixed-SST configuration, with SSTs set to the climatology taken from coupled runs of the same model and second, a 100-m-depth slab-ocean configuration, with surface fluxes derived from the fixed-SST configuration ([Table 3](#)). Both configurations are run with preindustrial carbon dioxide levels and fixed March boundary conditions (more on that shortly). One difference between these configurations is the sea ice model, which was fixed for the fixed-SST configuration and allowed to vary when using a slab ocean. This has been the main difference between the two configurations (aside from the obvious difference in heat capacity). Each configuration produced up to 100 years of data output sampled every 12 h.

We study the response to tropical SST perturbations. Two types of perturbations were considered: a simple Gaussian perturbation and realistic patterns derived from a coupled run of the same model at a finer resolution ([Santoso et al. 2012](#)). [Figure 1](#) shows the placement of the perturbations and [Table 1](#) lists the naming conventions by which these will be referenced. The realistic patterns used are the positive modes of the Indian Ocean dipole (IOD) and ENSO patterns, with the latter covering the entire Pacific Ocean between 30°N and 30°S. These patterns are realistic to the extent that they are produced by the same model and have a relation to the climatology on which the current simulations operate. They are nonrealistic in two ways: first, the patterns are specific to Mk3L and second, these are applied continuously for a duration of 30 years during which the simulation is run to equilibrium. We therefore refer to these patterns as ENSO-like and IOD-like patterns. The Gaussian patterns that were used were placed at the same locations as the realistic patterns (one in the Indian Ocean and two in the Pacific Ocean).

TABLE 2. The list variables used in the experiments. The column listing the number of components refers to the number of components or variance taken from each model level when reducing its dimensions at the first stage of the model reduction.

Variable ID	Description	No. of components or variance fraction	Dimensions
$T$	Temperature	600	3D
RH	Relative humidity	100	3D
$V$	Meridional wind speed	100	3D
$U$	Zonal wind speed	100	3D
$\omega$	Vertical velocity	100	3D
CRE(lw)	Longwave cloud radiative effect	0.9	2D
CRE(sw)	Shortwave cloud radiative effect	0.9	2D
CF(all)	Total-cloud fraction	0.9	2D
CF(high)	High-cloud fraction	0.9	2D
$P$ (all)	Total precipitation	0.9	2D
$P$ (conv)	Convective precipitation	0.9	2D

We verified that the simulation reaches approximate equilibrium in two ways: first, by ensuring that the difference between the means of relevant variables is approximately time invariant (perturbed simulation less control values) and, second, by looking at time series of the global means of these variables. In all simulations, including the slab-ocean simulations, the response of the system reaches approximate equilibrium within the first 10 years after the introduction of the perturbation.

Surface temperature perturbations such as ENSO and IOD are important forcing patterns interacting with the atmosphere. In contrast, FDT is applied to the atmosphere only. This required us to reinterpret the SST perturbations as an atmospheric forcing function defined on the model levels that are directly in contact with the surface. The forcing is defined as a temperature perturbation affecting the surface boundary layer and decaying toward the top of the boundary layer (which, for Mk3L, corresponds to the first five model levels). This is one potential source of errors that has to be taken into account when evaluating the results. However, at least for the tropics, it was found to be of lesser importance compared to other sources of error such as the model reduction approach and sample size.

*b. Construction of the operator*

Because of the dimensionality of a GCM, even at the relatively coarse Mk3L resolution, it is not practical to produce a response operator on the entire phase space of the system. As a result, one is forced choose a model reduction strategy—which introduces some bias. Our model reduction approach is adapted from the one that was used in GB07. The approach proposed in GB07 is unique in that it used a combination of variables—namely temperature and streamfunction—to construct a high-dimensional response operator. Motivated by the attempt to produce a proof of concept, GB07 did not

treat the two variables equally. The variables were normalized differently giving more emphasis to temperature. Streamfunction was reduced to the first 100 EOF components at each model level before reducing all the model levels of the two variables using a second EOF stage. From this second EOF reduction stage, the first 1800 components were used to accumulate lag covariances, from which the response operator was constructed. More recently, a similar approach using the same variables set was studied for the time-periodic (seasonal) case (Gritsun 2010). However, in that study the phase space of the climate system was first interpolated to two vertical levels ( $\sigma = 0.336$  and  $0.664$ ). As a consequence, the forcing function may not be unique; that is, two forcing functions with different responses may have the same reduced representation. Using only two vertical levels also means that the study of the response is limited to those levels (the paper only presents the response of streamfunction at  $\sigma = 0.336$ ). A key difference in this work, compared to the ones discussed so far (i.e., GB07; GBM08; Gritsun 2010), is in that the sample size used to construct the operator is significantly smaller and the derivation of the operator is forced to take that into account.

Seeking to explore the skill of high-dimensional operators, while consolidating the approach used in GB07, we implement several changes:

- (i) First, all the variables that were used were normalized at each model level by removing the area-weighted standard deviation of the respective model level. There was no favoring of one variable over another at this stage (i.e., weighting).
- (ii) Each model level (and for each variable) is then transformed to an EOF basis. The variables used and the number of components kept at each model level is listed in Table 2. For temperature, 600 EOF components were kept in order to properly represent

the forcing function. This represented approximately 97.5% of the variance at each model level. For other variables, 100 EOF components were kept, which represented approximately 90% of the variance at each model level. This stage will be referred to as the first reduction stage. An exception to this was relative humidity for which 100 components at each model level amounted to 60%–70% of the variance. Adding more components of this variable was not possible because of the long tail of variance and the limitations imposed by the relatively small sample. Reasons to consider relative humidity as part of the state variables will be discussed shortly.

- (iii) The reduced variables at all model levels are then stacked and a second EOF reduction phase is carried out. It was found that keeping enough components at this stage to capture 90% of the variance produced the highest skill. This amounted to 800–2000 components, depending on the variable combination that was selected.
- (iv) Using the components taken at the second EOF reduction stage, lag covariances are calculated for up to 30 days.

The limiting factor guiding this approach is the lack of sample, which affects the reduced representation. Errors due to reduced representation can be divided into errors due to representation of the forcing and errors due to representation of the state. We note that the early truncation of temperature components, imposed by lack of sample, results in a violation of the prerequisites of a reduced representation described in [Majda et al. \(2010, their section 2b\)](#). This is due to the fact that the forcing is not perfectly captured by the reduced representation.

We start by discussing the representation of the forcing; a key problem with the approach presented above is capturing “unnatural” or highly localized perturbation patterns. The operator is constructed using historical data, and the perturbation pattern may only occur at small amplitudes in the natural variability. It is essential to ensure that such patterns are properly represented after the model reduction phase. The perturbations used here, and in [GB07](#), tend to project to low-order components of the lower model levels. This creates a conflict between the need to represent the perturbation and errors attributed to components with low variance ([Martynov and Nechepurenko 2006; GB07](#)).

To demonstrate this issue, we project the Gaussian pattern centered at  $0^\circ, 165^\circ\text{W}$  onto the EOF basis of the lowest model level. This is done using 300 and 600 components that capture, respectively, about 90% and

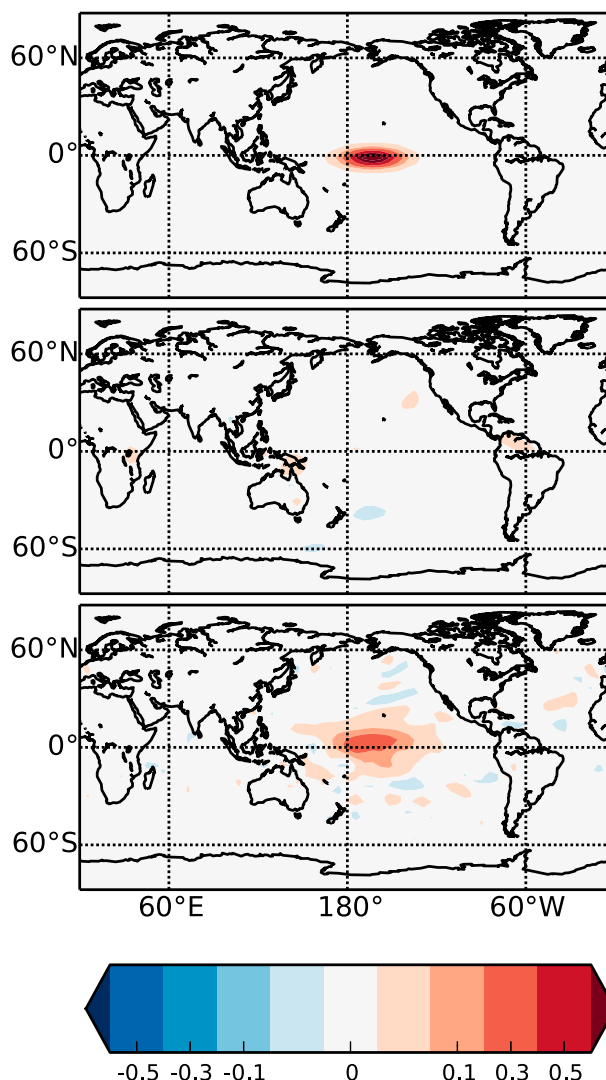


FIG. 2. (top) The results of transforming the central Pacific Gaussian SST perturbation pattern onto the reduced basis of the first (lowest) model level of the fixed-SST case. (middle), (bottom) As in the top panel, but using 300 (~90% variance) and 600 components (~97.5% variance), respectively.

97% of the variance. The top panel in [Fig. 2](#) shows the original pattern; the results of the projection to and from the two bases are plotted in the middle panel (300 components) and bottom panel (600 components). Looking at the middle panel, it is apparent that the forcing pattern is mostly represented by the lowest 10% of the variance. In addition, comparing the top and the bottom panels, it is apparent that the lowest 2.5% of the variance is needed to fully capture the amplitude of the pattern (which in this case was 1 K). However, going beyond the 97.5% variance per model level was found to decrease the skill of the operator. As a consequence, for patterns that project poorly onto the natural variability,

such as the Gaussian SST perturbation in the eastern Pacific, this approach is not sufficient to capture the pattern. Since some form of model reduction is inevitable in these settings, this analysis proves to be an essential step in applying this approach to climate scenarios.

For the other patterns tested, keeping 600 components at each model level in the first reduction stage was sufficient to reproduce the pattern of the response (Fig. 3). On the other hand, the amplitude of the response was, in general, smaller than the true response. A natural assumption is that the loss of amplitude in the response is proportional to the loss of amplitude in the forcing owing to the model reduction. This assumption is especially justified if the operator is successful in reproducing the pattern (but not the amplitude). However, we were not able to find a simple scaling relation to account for the lost amplitude. This relation becomes more complicated once multiple variables, excluded from the forcing pattern, are used. We therefore focus on the skill of the operator in reproducing the spatial pattern of the response. In what follows, both the true and estimated responses were standardized to unit variance.

Next, we discuss the representation of the state. The use of relative humidity required some consideration. The incentive for its inclusion comes from several reasons. First, this choice is physically motivated, since the thermodynamic state of the climate system is better represented by the inclusion of water vapor. It is well established that information on current humidity improves the accuracy of weather forecasts (e.g., Chahine et al. 2006; Benjamin et al. 2010). Relative humidity was preferred over other variables associated with water vapor since it is less dependent on temperature and shows relatively constant variance (across model levels and compared to other state variables). Second, we wish to study the prediction of cloud response, and inclusion of direct information about water vapor is generally considered more relevant in this case. Third, humidity displays a fine spatial structure that tends not to be captured by temperature and wind. It is assumed that the leading components of relative humidity replace some of the long tail of truncated temperature components. This is particularly important when seeking a reduced representation in a small sample, which forces us to perform a two-step model reduction. Finally, one cannot rule out the possibility that a heuristic search of the space of possible reductions would yield a skillful operator.

As a metric of evaluation we choose spatial pattern correlations. This metric is sensitive to shifts, translations, and rotations of patterns. To account for that, the patterns were also manually inspected. In addition, confidence intervals were computed to ensure the significance

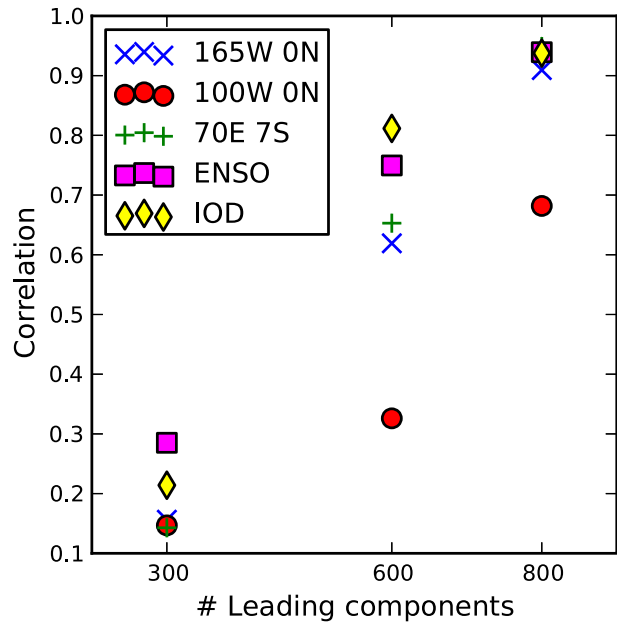


FIG. 3. The skill in reproducing the true forcing (in terms of pattern correlation) as a function of the number of temperature components retained at the bottom model level, where the perturbation is applied, for the fixed-SST case.

of the correlations. The use of relative entropy as a metric was also considered as an alternative to correlations, but this metric suffers from the same pointwise biases as correlations and is only usable to compare one prediction against another.

### 3. Results

In this section we study the relationship between the spatial dimensions of an operator, the sample size from which an operator is fitted, and its skill. Two key aspects are investigated. First, we investigate the skill as a function of the number of retained EOF basis components and state variables that are included in the model reduction. As will be seen, the choice of a sufficient number of features is intimately related to the ability of the model reduction technique to represent the climate state and imposed perturbation. Second, we investigate the relation between the skill and sample size when the sample size is well below an ideal sample (e.g., GB07; Gritsun 2010) and approaching the dimensionality of the operator. In what follows, unless otherwise specified, the results correspond to an operator that is constructed based on no more than 100 years of control run sampled at 12-h intervals.

#### a. Dependence of results on the perturbation

We start by studying the skill of a univariate, temperature-based operator in reproducing equilibrium

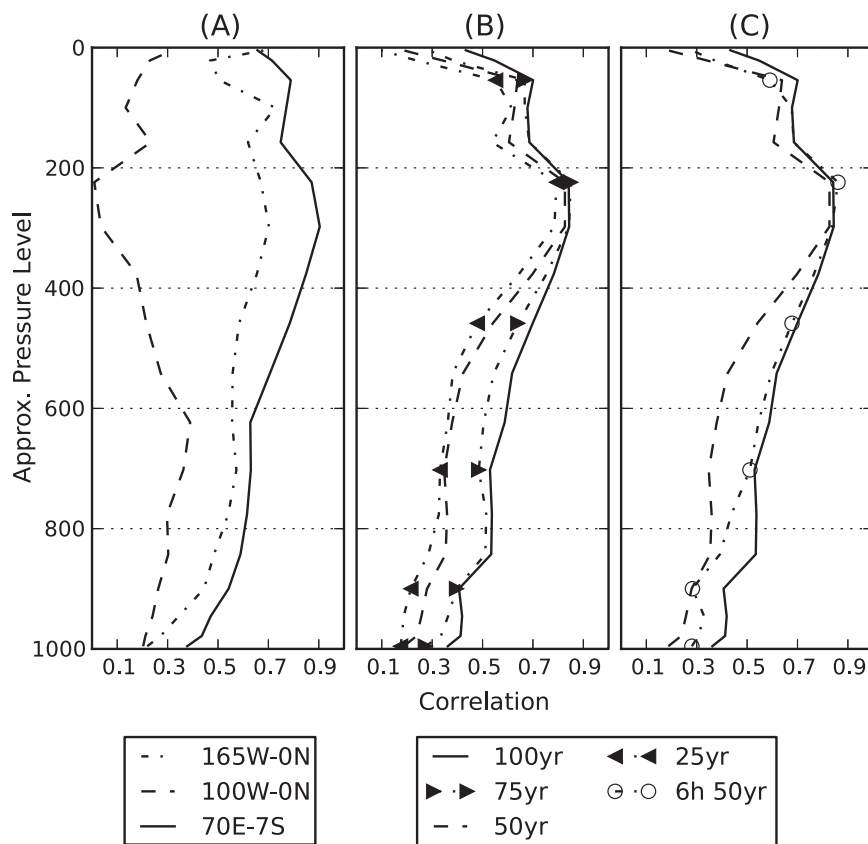


FIG. 4. Pattern correlations comparing true and predicted responses for the fixed-SST cases. Comparing the responses to (a) Gaussian SST forcing at different locations, (b) operators constructed from different sample sizes, and (c) sampling rates. Refer to the text for further information.

responses to the Gaussian SST perturbations. Figure 4a shows the skill of the operator in predicting the response to the local Gaussian perturbations, described in Table 1, in terms of pattern correlation at each model level. Most notable are the differences in skill among perturbation scenarios. The highest global skill is achieved for the Indian Ocean perturbation ( $7^{\circ}\text{S}$ ,  $70^{\circ}\text{E}$ ). The pattern correlation is moderate for the central Pacific perturbation ( $0^{\circ}$ ,  $165^{\circ}\text{W}$ ) and low for the eastern Pacific perturbation ( $0^{\circ}$ ,  $100^{\circ}\text{W}$ ). An inspection of the patterns at different pressure levels (not shown) suggests that the modest reduction in skill for the central Pacific perturbation arises mainly from errors in the Indian Ocean region.

The possibility that the lack of skill of the operator in the eastern Pacific case is related to the sampling rate was ruled out by changing these parameters in the simulation. We also ruled out nonlinear responses as a primary cause by running the same set of simulations with an inverted (cooling) pattern, taking the center difference of the warming and cooling as the linear response (as was done in GB07). On the other hand, as was noted

above, the perturbation pattern in the eastern Pacific case was significantly less well preserved than the other perturbations at the model reduction phase (Fig. 3). Note that the ordering of the 600 components in Fig. 3 is highly correlated to the skill in predicting the response. We believe this is a leading possibility for explaining the poor performance for this case.

#### b. Addition of variables

Including temperature as part of the operator is essential because the external forcing consists of heating. One motivation to introduce additional variables is the possibility of increasing the skill of the operator, as was done in GB07. Another motivation is the need to study a certain set of variables. In general, the amount of skill gained by introducing a variable represents an information content that may be related to a process that was not captured previously, motivating the study of operators consisting of different variable combinations.

We study the increase in dimensionality by inclusion of additional variables using the realistic SST perturbation

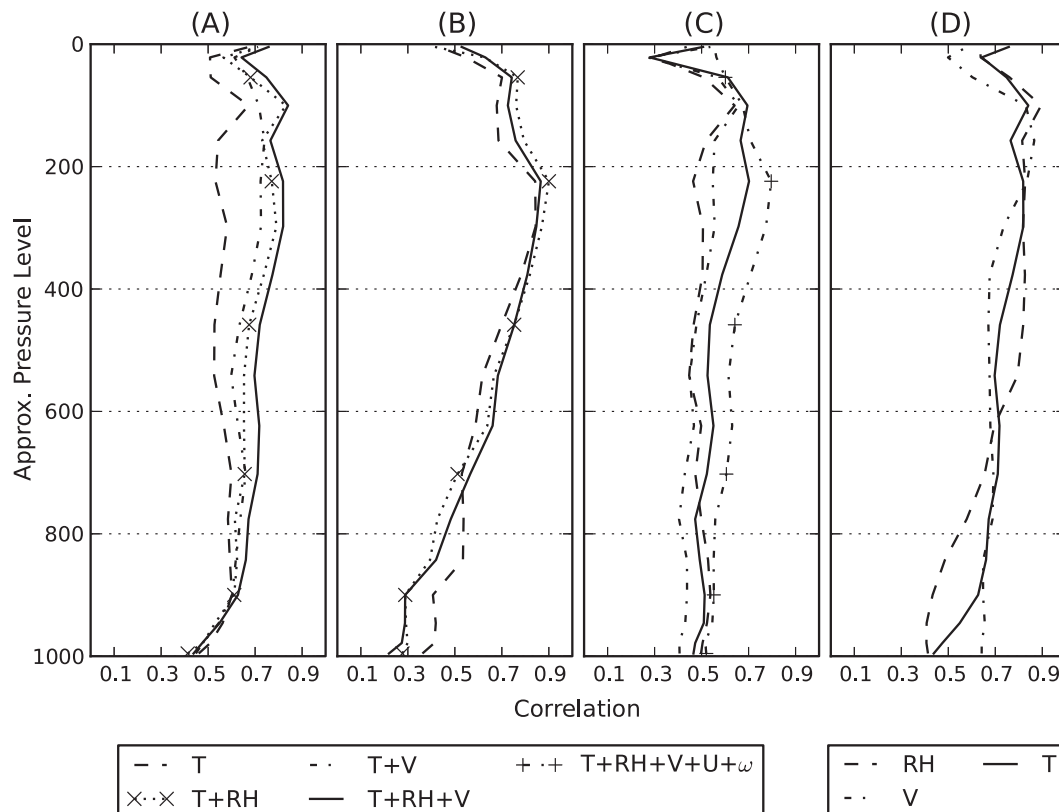


FIG. 5. Pattern correlations comparing true and predicted temperature responses of operators of growing complexity to (a) ENSO-like perturbation and (b) IOD-like perturbation for the fixed-SST case. (c) Repeating (a) with the addition of a slab ocean. (d) Comparing the true and predicted responses for RH and  $V$  using the  $(T + RH + V)$  operator to the ENSO-like perturbation for the fixed-SST case. Refer to the text for further information.

scenarios. Figures 5a and 5b show the temperature pattern correlations for the ENSO-like and the IOD-like perturbations, respectively, for different operators. To demonstrate the relation between the skill of the operator and the information gained from a specific variable, the plots present a sequence of operators of growing complexity. These include temperature, relative humidity, and meridional wind (refer to Table 2 for more details). The zonal wind component was excluded from the operators since it degraded the skill of the operators, while vertical velocity did not add skill. The skill in the IOD-like case is similar to the Gaussian case at the same location (Fig. 4a), perhaps because the two patterns are similar in size and location. The correlations in the free troposphere are fairly high with one variable and therefore adding more variables does not improve much on the univariate case. However, the improvements are still significant at the 95% confidence interval. For the ENSO-like perturbation, there is a smooth increase in skill for temperature as more variables are introduced to the operator. An inspection of the pattern of the response suggests that the

improvement is attributed to added skill over the Indian Ocean (not shown).

So far, even though we used multivariate operators, only the skill of temperature patterns was evaluated. But, adding more variables to the operator allows us to study the response of these variables as part of the state. In the current example, the operator was augmented with relative humidity (RH) and meridional velocity  $V$ . It was found that the skill in estimating these variables closely matched the skill of temperature. For example, the first three rows in Fig. 6 compare the true and predicted the responses of  $T$ , RH, and  $V$  for the full  $(T + RH + V)$  operator at 700 hPa to ENSO-like perturbation. The correlation at this level is about 0.69, peaking around 0.85 at 100 hPa (Fig. 5d). In some cases, adding one variable improved the skill of another; for example, meridional velocity improved the skill for relative humidity. We attribute this to improved numerical properties of the operator that includes all variables compared to the one that includes only temperature and relative humidity. This was observed by looking at the eigenvalues of the lag-zero covariance matrix of each operator

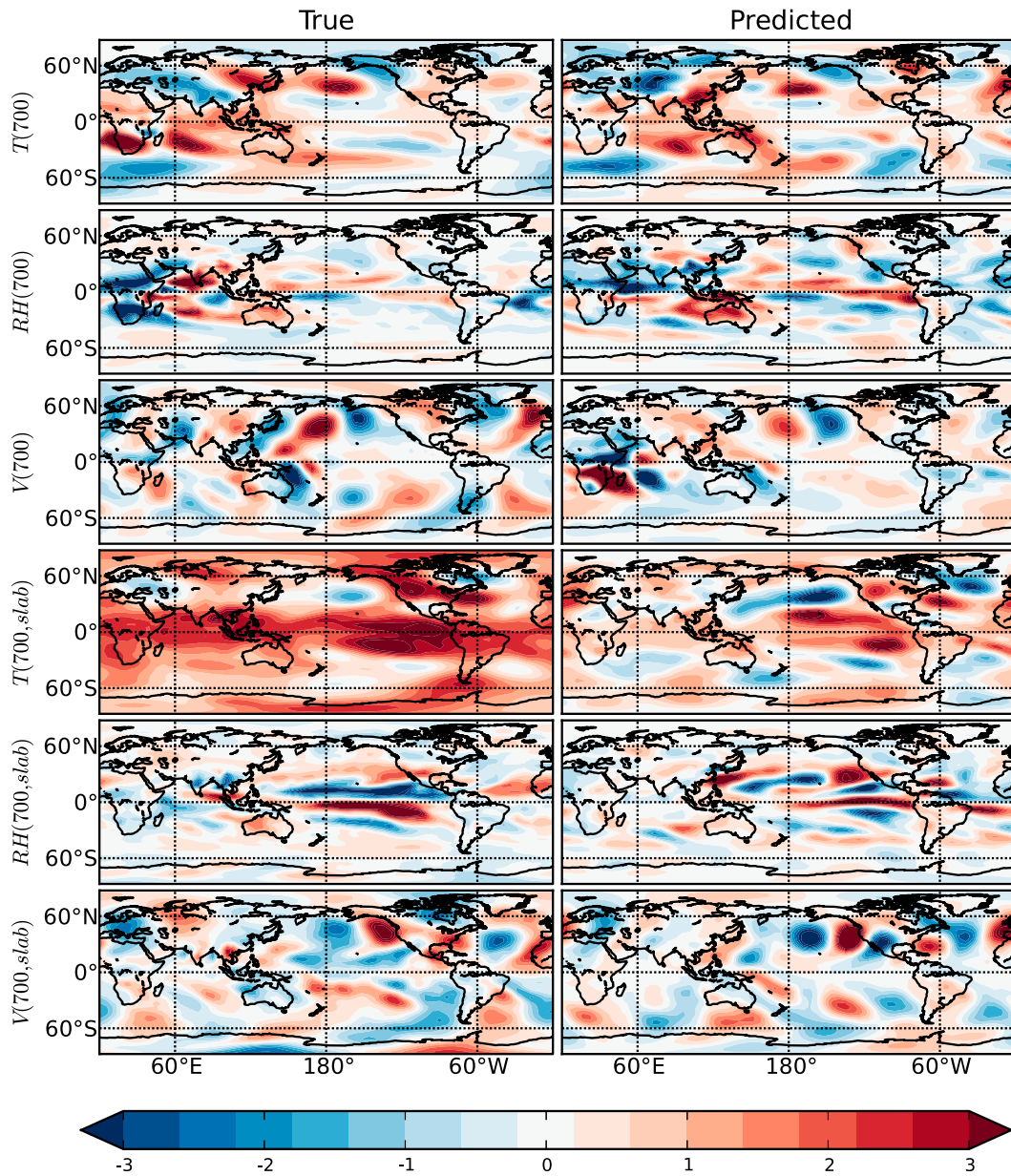


FIG. 6. Comparing the responses at 700 hPa for  $T$ ,  $RH$ , and  $V$  to an ENSO-like perturbation (standardized) for (top three rows) the fixed-SST scenario and (bottom three rows) the slab-ocean scenario.

[as described in [Martynov and Nechepurenko \(2006\)](#) and [GB07](#)].

### c. Estimating cloud response

Next, we examine the skill of operators in estimating the cloud response. [GBM08](#) demonstrated by example that the FD operator has skill in estimating variables with known or assumed functional relationship to the variables that compose the operator. This idea has been discussed by both [Leith \(1975\)](#) and [Majda et al. \(2005\)](#) (although using different arguments as justification). In

the current model setup, where the seasons and ocean are fixed, clouds are emphasized as a driver of variability. Therefore, it is expected that an operator will capture important relations between cloud variables and variables representing the climate state. Furthermore, working with multiple operators consisting of different sets of variables offers the opportunity to study these relations as a function of different representations of the climate state. From this perspective, the lack of skill of an operator is as important as the presence of skill.

Figure 7 shows the pattern correlations and absolute errors for six quadratic measures related to cloud or precipitation for four different operators. The correlation increases as more variables are introduced to the operator, and the absolute error decreases, consistent with the skill for the operator quantities themselves. For the shortwave cloud radiative effect [CRE(sw)] and precipitation  $P$ , the correlation is generally low, with slight improvement when adding variables to the operator. The pattern maps, however, show that, even for these variables, the operator captures the main geographic features of the response, with much of the error arising from small-scale details that are not reproduced (Fig. 8). This feature points to the limitation of using any kind of point by point correlations as a measure for success. For example, for the  $(T + RH + V)$  operator, the correlation of shortwave CRE is 0.55 while longwave CRE is 0.78. However, from Fig. 8 it is apparent that both show skill and the difference in skill is not easy to discern.

Once a multivariate operator achieves high skill in reproducing a cloud variable, one can assume that it captures the climate process. It is then possible to use the operator to attribute the skill contribution to the different state variables. We demonstrate this on convective precipitation [ $P(\text{conv})$ ] and high-cloud fraction [CF(high)]. Figure 9 shows this idea for CF(high) where the contributions of relative humidity and meridional velocity are separated from that of temperature. The bottom-right plot shows the difference of results with operators  $(T + RH + V)$  versus  $T$ . Relative humidity and meridional velocity increase the skill in the Indian Ocean, consistent with the fact that temperature alone did not show skill there (for this perturbation). The response in the Pacific stretching to the Gulf of Mexico is also mostly related to these additional variables. For  $P(\text{conv})$  the response in the Indian Ocean follows the same lines as for CF(high) (Fig. 10). In addition, most of the response in the South Pacific convergence zone (SPCZ) and around the Maritime Continent can be attributed to relative humidity and meridional velocity. These results demonstrate the value in using this method to condition a climate response as a function of specific state variable. Note, however, that in order to achieve complete separation one is required to produce operators for the entire power set of variables included in the original (full skill) operator.

One critique of this approach is that the guarantees provided by FDT rely on the complete state vector of the system, while using subsets of variables from the full operator does not benefit from those guarantees. In previous sections, the argument for incorporating a subset of variables in the state vector was that it provides sufficient skill (i.e., other climate variables are superfluous). What is

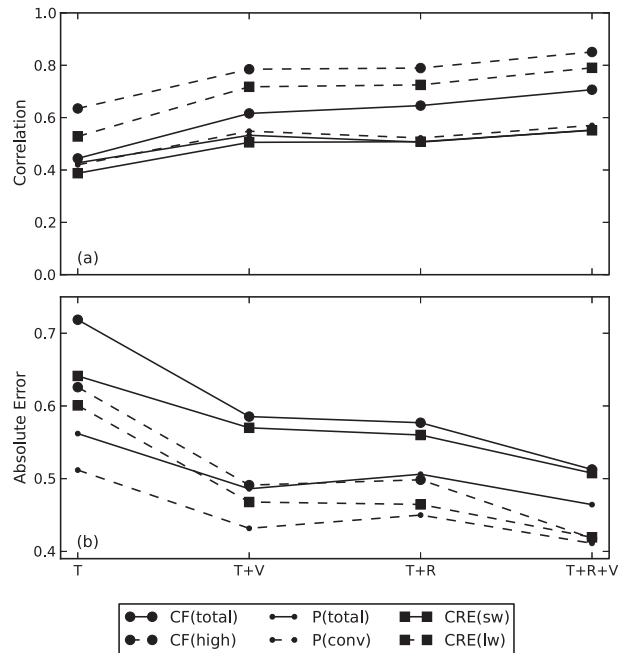


FIG. 7. Correlations and absolute errors of six cloud-related variables as a function of the operator that was used for the fixed-SST case.

then the argument supporting subsets of variables when the skill may be affected? If we look at the covariance matrix, from which the operator is constructed, removing a variable is equivalent to zeroing of matrix elements where that variable occurs. Assuming that the errors that are introduced are small, the loss of skill is associated with information that exists only in the excluded variable (and not in other variables that are included in the operator).

*d. Addition of interactive SST via a slab ocean*

So far surface perturbations were used as external forcing but the surface temperature was held fixed. We now remove part of this limitation by adding a mixed-layer (slab) ocean, so as to allow more natural temperature variability at the surface. A new set of operators is constructed using 100 years of control runs that include a slab ocean and fluxes derived from the fixed-SST control runs. The perturbation patterns in this case remain the same but these are now applied as prescribed heating rates to the slab ocean ( $\text{K day}^{-1}$ ). For comparative purposes, we ensure (through trial and error) that the magnitude of the temperature response pattern at the surface matches the magnitude that was imposed in the fixed-SST case (mean values). The perturbed simulations are again run for 30 years to equilibrium.

The first question to ask is whether the same combination of variables, optimal in the fixed-SST scenario,

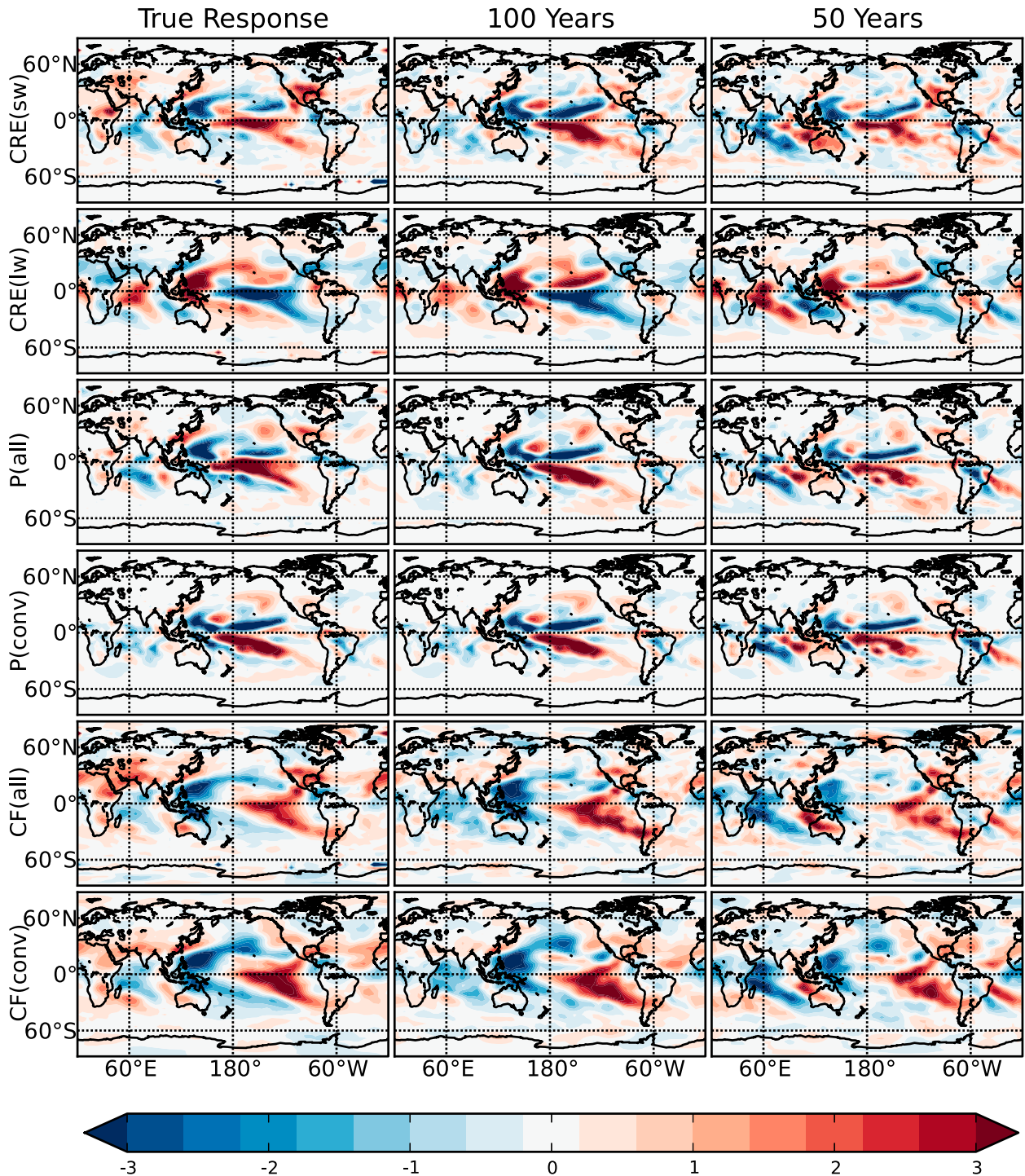


FIG. 8. Comparing true and predicted responses of several cloud-related variables to an ENSO-like perturbation using (left) the  $(T + RH + V)$  operator and (middle) 100 and (right) 50 years of data for the fixed-SST case.

will also produce the highest skill here. Figure 5c shows the pattern correlation of various operators tested. The operator that produced the highest skill in the fixed-SST case ( $T + RH + V$ ) did not achieve the highest skill here.

The zonal wind component that was excluded from the fixed-SST case since it degraded the skill of the operator (possibly owing to colinearities with temperature) was found to add skill in the slab-ocean case. Interestingly, it

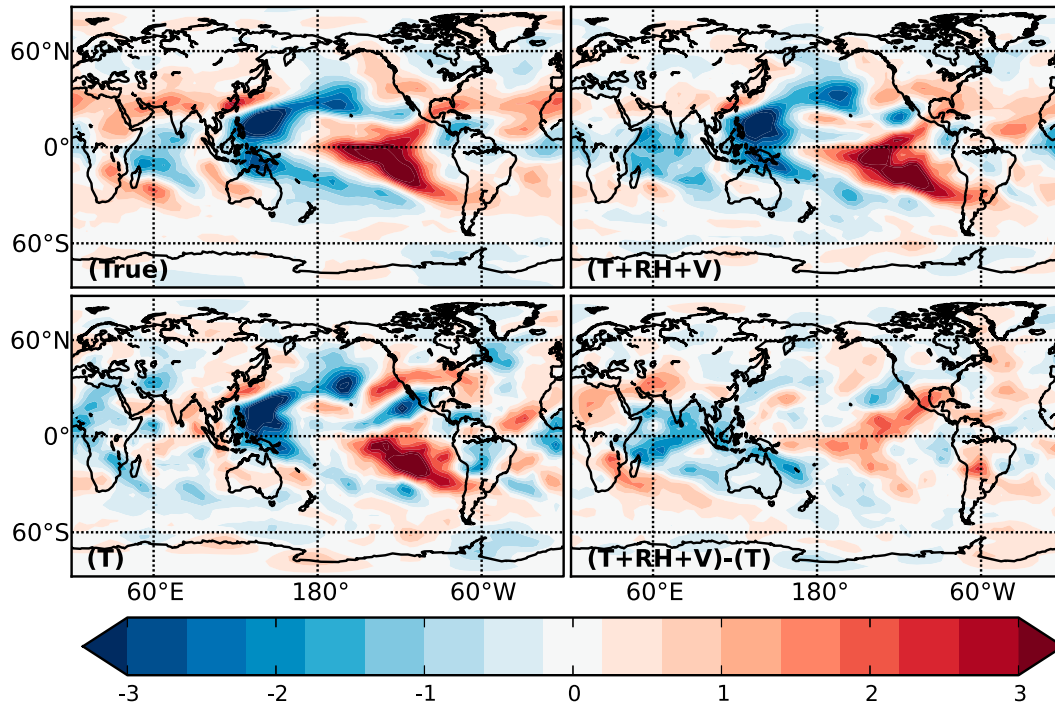


FIG. 9. CF(high) response to ENSO-like perturbation (standardized). Separating the response due to relative humidity and meridional velocity from temperature.

was essential to include vertical velocity to bring the skill to acceptable levels, as seen for the operator  $(T + RH + U + V + \omega)$ . A closer look at the differences between the standardized estimates of the  $(T + RH + U + V + \omega)$  and  $(T + RH + V)$  operators showed some differences in skill in the Indian Ocean, Europe, and southern midlatitudes (not shown). Overall, qualitatively, both operators had similar responses. However, the squared-error difference between the true response and the estimated responses of both operators shows a 40% improvement for the full operator  $(T + RH + U + V + \omega)$ .

An important difference in the behavior of the operator in the slab-ocean scenario compared to the fixed-SST scenario was the temperature response. The perturbed slab simulations allowed the mean temperature to drift further away from its control values. We found that the magnitude of the predicted temperature response was about a third of the true response (fourth row in Fig. 6). This was the case only for temperature and was partly alleviated as more variables were introduced to the operator. We assume that part of this difference can be attributed to missing temperature components in the operator's state representation. Other variables used in the operator did not show this bias (bottom two rows in Fig. 6).

*e. Relation of skill to sample size*

We now focus on the relationship of the skill to the sample size or record length. Validation of the FD

approach for the climate case has so far focused either on asymptotic bounds or on idealistic settings with 10 000 years of data (i.e., GB07). The relation between the sample size to the increase in errors has been shown to be asymptotically proportional to  $1/\sqrt{N}$ , where  $N$  is the sample size (Martynov and Nechepurenko 2006). The short duration of useful climate records justifies looking at the lower bounds of the problem, since, ideally, one would want to produce FDT operators from observed data. In this section the data are taken from the same fixed-SST simulation that produced 100 years of data, from which the results shown so far were produced. From these data, we produce operators for 75, 50, and 25 years beginning at arbitrary starting points in the simulation (Table 3).

One thing that needs to be taken into account when looking at the lower bounds of the sample size is the relation between the dimensionality of the problem and the sample size. A hard lower bound on the sample size is the number of components needed to construct a skillful operator without the problem becoming underdetermined. The dimensionality of the operators produced so far was well below 2000 components. However, another bottleneck that needs to be considered is the requirements of the model reduction approach that is used. For example, the selection of 100 years of simulation to construct the operators amounts to a sample size  $N = 73\,000$ , which is only slightly larger than the dimensionality of a single atmospheric variable in Mk3L

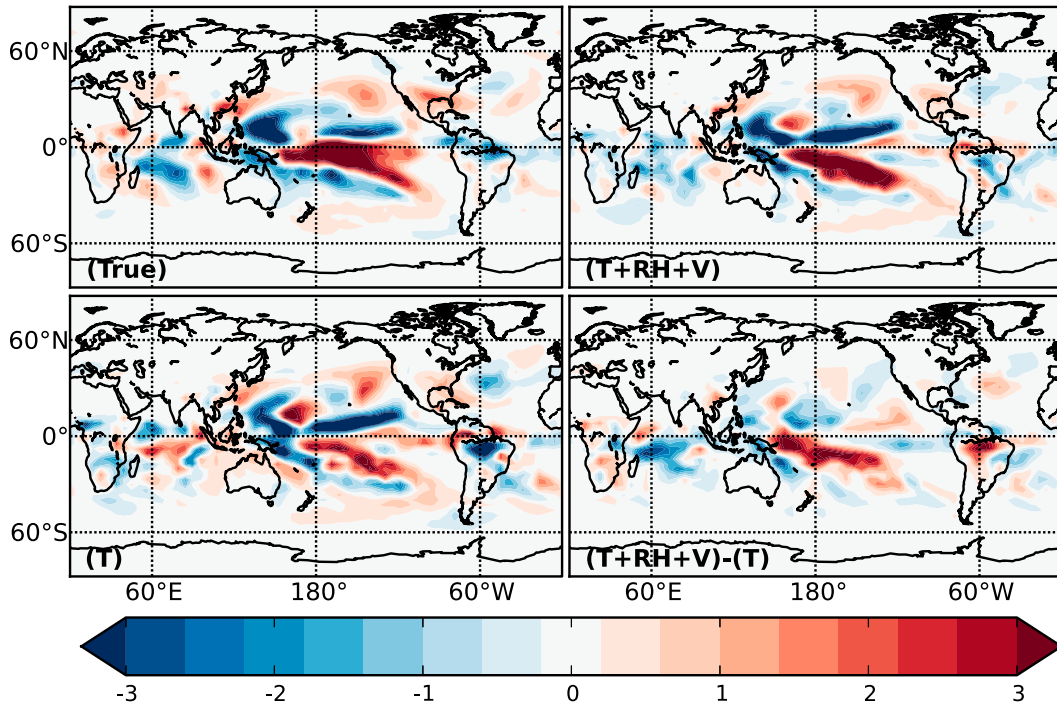


FIG. 10. As in Fig. 9, but for  $P(\text{conv})$  response to ENSO-like perturbation (standardized). Separating the response due to relative humidity and meridional velocity from temperature.

(3D grid size = 64 512). Our procedure of first transforming each model level to a reduced EOF basis partly circumvents this.

Figure 4b shows the pattern correlations, comparing the responses for the IOD-like perturbation, for a suit of operators constructed using 100–25 years of data. It is apparent that the skill depends on sample size. Interestingly, the degradation in skill is small in the mid- and high troposphere where the skill is high. Similar behavior was observed with the other patterns that were studied. Qualitatively, the degradation in skill was away from the source of the perturbation. For 50 years of data, several samples were drawn from the 100-yr simulation, and operators were constructed using these samples. The predictions and skill of these operators were compared and found to be equivalent. One option that was explored was the relation of the skill to a change in the sampling rate. Figure 4c compares the pattern correlations for predictions made by operators that were constructed using 100 and 50 years of data sampled at 12-h intervals and 50 years of data sampled at 6-h intervals. Note that the sample size for the latter matches the sample size of the 100-yr run at 12-h intervals. In this case, the improvement in skill due to sampling brings the skill of a 50-yr operator closer to the 100-yr operator.

Similar relationships between skill and sample size were observed for operators predicting cloud responses.

While degradation in skill due to a decrease in sample size was visible, the main features of the cloud response are present. For example, in Fig. 8, the response of the longwave cloud radiative effect [CRE(lw)] is well reproduced by both 100- and 50-yr-based operators. However, for the 50-yr-based operator, there is a spurious response in the Atlantic Ocean (away from the imposed ENSO-like perturbation). In contrast, for precipitation, there is a visible decrease in skill in the Pacific. Overall, while the increase in errors is clearly visible, the core of the prediction was maintained. This was the case even for a variable such as CRE(sw), where the correlations were generally low.

#### 4. Discussion

This paper investigates the skill of FD operators and its dependence on dimensionality and sample size. The

TABLE 3. Main simulation parameters.

Simulation	Purpose	Duration (yr)
Control (fix SST)	Construct FD operator	100, 75, 50, 25
Control (slab ocean)		
SST forcing (fix SST)	Evaluate FD response	30
SST forcing (slab ocean)		

working hypothesis guiding this work was that increasing the dimensionality and broadening the choice of climate variables could substantially improve the performance of FD operators for climate applications. Ocean surface temperature patterns were investigated as a source of external forcing of the atmosphere, as opposed to more idealized forcings used in previous studies (i.e., GB07; Ring and Plumb 2008; Gritsun 2010). The skill of the operators in reproducing responses to such perturbations was shown to differ when the surface is treated as a slab ocean compared to the case where surface temperatures remains fixed. In particular, with a slab ocean, a more extended set of variables was found to produce the highest skill. Interestingly, in this case, the inclusion of vertical velocity was essential to the skill of the operator, possibly because of the larger natural fluctuations of this variable in the control climate when SST is variable. The immediate consequence of a variable SST was an increase in the dimensionality required in order to achieve skillful operators.

The results suggest that the FD operator is more skillful in estimating the response to realistic patterns than to highly localized “hot spots.” The highest skill was indeed achieved for ENSO-like perturbation patterns. This was despite the fact that the operator was produced from model runs where ENSO did not explicitly occur. The fact that these patterns achieved high skill, while other patterns on the same geographical location achieved low skill, implies that a fundamental change in surface patterns may decrease the skill of an FD operator. It also points out the importance of the surface as an external forcing of the atmosphere and in determining the atmospheric response. However, it should be noted that, in order to reach a greater degree of confidence in these results, more extensive experiments are required. Another limitation of this study comes from the fact that only the response to perturbations that are reliably described in the reduced basis of the operator can be predicted in this approach.

Another aspect put to the test here is the use of the theory under conditions that approximate practically available observations. As was demonstrated by Kirk-Davidoff (2009), success of the theory with arbitrarily large sample sizes may not indicate practical utility. We studied the lower bounds of the sample size, relating it to the spatial dimensionality of the operator and the data requirements of the model reduction technique that was used. We show that even in the extreme conditions, where the sample size approaches the hard lower bound below which the problem becomes ill posed, an FD operator based on the quasi-Gaussian assumption (Majda et al. 2005) still has skill in reproducing climate responses. Despite clear degradation of skill in relation to sample

size, the main features of the response persisted as the sample size was shrunk. The relation between sample size and the dimensionality of the operator prevents further reduction in the sample size. One possible extension to the current approach is to replace the naive model reduction approach used here by more elaborate strategies. For example, Cooper et al. (2013) proposed to replace the selection of a reduced basis based on leading EOFs with a greedy algorithm based on the spatial locality assumption. Such approaches may result in improved performance of the FD operator. In the current approach, the dependence of skill on the choice of state variables suggests that proper choice of variables can mitigate lack of data. Furthermore, it is important to identify those subsets of variables and features that produce skillful operators under conditions that approximate real observation.

For cloud variables, the operator was able to capture the key features of the responses. Although a decrease in skill with shortening sample size was visible, gross features of the response were captured even with 50 years of data and some still evident with shorter records. These record lengths are within what is now available from the satellite record beginning in 1979. Since the time scale of the forcing defined by FDT matches the time scale of cloud processes, FDT is an ideal framework to study these processes. One application that was demonstrated here was the ability to study cloud responses as a function of different FD operators (encapsulating different climate-state representations). This allowed us to separate the response due to temperature from those of relative humidity and meridional velocity. A more complete separation of responses can be achieved by considering the power set of variables found in the operator.

Looking beyond this work, we note challenges and opportunities on the path to an operator that is derived from observations. Among the challenges are measurement errors, missing data, and seasonality (Majda 2012). Formal quantification of the error term due to missing data and measurement error is required. Seasonality may fragment the observed sample into subsets of distributions with an approximately Gaussian PDF (Majda and Wang 2010). However, the interpretation offered by Gritsun (2010) may be overly restrictive since our knowledge of the climate system suggests a smoother day-to-day variability (hence a smaller degree of fragmentation may be required). Combined with a dynamical ocean, seasonality also ensures a wider set of perturbations will be part of the natural variability, making the lack of skill to warming in the eastern Pacific less probable. In terms of representation, the approach offered here is clearly not the end of the road. Approaches that take advantage of specific assumptions related to the

representation of the state and forcing (e.g., Cooper et al. 2013; Majda et al. 2010) may improve the skill of the operator while further reducing the lower bounds of the sample size.

In a broader sense, FDT tests the limits of our understanding of climate. Because of the complexity and nonlinearity of climate, the theory can at best work only approximately, but this may be enough for it to have utility. It is crucial to establish our confidence in those approximations that show high skill. Application of the theory to arbitrary sample sizes and feature sets is discouraged.

*Acknowledgments.* The authors thank G. Branstator for providing important comments that helped improve earlier versions of this manuscript. In addition, we thank S. J. Phipps for his assistance and countless discussions concerning the Mk3L model.

#### REFERENCES

- Abramov, R. V., and A. J. Majda, 2007: Blended response algorithms for linear fluctuation-dissipation for complex nonlinear dynamical systems. *Nonlinearity*, **20**, 2793, doi:10.1088/0951-7715/20/12/004.
- Baiesi, M., and C. Maes, 2013: An update on the nonequilibrium linear response. *New J. Phys.*, **15**, 013004, doi:10.1088/1367-2630/15/1/013004.
- Bell, T. L., 1980: Climate sensitivity from fluctuation dissipation: Some simple model tests. *J. Atmos. Sci.*, **37**, 1700–1707, doi:10.1175/1520-0469(1980)037<1700:CSFFDS>2.0.CO;2.
- Benjamin, S. G., B. D. Jamison, W. R. Moninger, S. R. Sahn, B. E. Schwartz, and T. W. Schlatter, 2010: Relative short-range forecast impact from aircraft, profiler, radiosonde, VAD, GPS-PW, METAR, and mesonet observations via the RUC hourly assimilation cycle. *Mon. Wea. Rev.*, **138**, 1319–1343, doi:10.1175/2009MWR3097.1.
- Chahine, M. T., and Coauthors, 2006: AIRS: Improving weather forecasting and providing new data on greenhouse gases. *Bull. Amer. Meteor. Soc.*, **87**, 911–926, doi:10.1175/BAMS-87-7-911.
- Cionni, I., G. Visconti, and F. Sassi, 2004: Fluctuation dissipation theorem in a general circulation model. *Geophys. Res. Lett.*, **31**, L09206, doi:10.1029/2004GL019739.
- Colangeli, M., and V. Lucarini, 2014: Elements of a unified framework for response formulae. *J. Stat. Mech.*, **2014**, P01002, doi:10.1088/1742-5468/2014/01/P01002.
- , L. Rondoni, and A. Vulpiani, 2012: Fluctuation-dissipation relation for chaotic non-Hamiltonian systems. *J. Stat. Mech.*, **2012**, L04002, doi:10.1088/1742-5468/2012/04/L04002.
- Cooper, F. C., and P. H. Haynes, 2011: Climate sensitivity via a nonparametric fluctuation–dissipation theorem. *J. Atmos. Sci.*, **68**, 937–953, doi:10.1175/2010JAS3633.1.
- , J. G. Esler, and P. H. Haynes, 2013: Estimation of the local response to a forcing in a high dimensional system using the fluctuation-dissipation theorem. *Nonlin. Processes Geophys.*, **20**, 239–248, doi:10.5194/npg-20-239-2013.
- Gritsoun, A. S., G. W. Branstator, and V. P. Dymnikov, 2002: Construction of the linear response operator of an atmospheric general circulation model to small external forcing. *ESAIM: Math. Modell. Numer. Anal.*, **17**, 399–416.
- Gritsun, A. S., 2010: Construction of response operators to small external forcings for atmospheric general circulation models with time periodic right-hand sides. *Izv., Atmos. Ocean. Phys.*, **46**, 748–756, doi:10.1134/S000143381006006X.
- , and G. Branstator, 2007: Climate response using a three-dimensional operator based on the fluctuation–dissipation theorem. *J. Atmos. Sci.*, **64**, 2558–2575, doi:10.1175/JAS3943.1.
- , —, and A. Majda, 2008: Climate response of linear and quadratic functionals using the fluctuation–dissipation theorem. *J. Atmos. Sci.*, **65**, 2824–2841, doi:10.1175/2007JAS2496.1.
- Kirk-Davidoff, D. B., 2009: On the diagnosis of climate sensitivity using observations of fluctuations. *Atmos. Chem. Phys.*, **9**, 813–822, doi:10.5194/acp-9-813-2009.
- Leith, C. E., 1975: Climate response and fluctuation dissipation. *J. Atmos. Sci.*, **32**, 2022–2026, doi:10.1175/1520-0469(1975)032<2022:CRAFD>2.0.CO;2.
- Majda, A. J., 2012: Challenges in climate science and contemporary applied mathematics. *Commun. Pure Appl. Math.*, **65**, 920–948, doi:10.1002/cpa.21401.
- , and X. Wang, 2010: Linear response theory for statistical ensembles in complex systems with time-periodic forcing. *Commun. Math. Sci.*, **8**, 145–172, doi:10.4310/CMS.2010.v8.n1.a8.
- , R. V. Abramov, and M. J. Grote, 2005: *Information Theory and Stochastics for Multiscale Nonlinear Systems*. CRM Monogr. Series, Vol. 25, American Mathematical Society, 133 pp.
- , B. Gershgorin, and Y. Yuan, 2010: Low-frequency climate response and fluctuation–dissipation theorems: Theory and practice. *J. Atmos. Sci.*, **67**, 1186–1201, doi:10.1175/2009JAS3264.1.
- Martynov, R., and Y. Nechepurenko, 2006: Finding the response matrix to the external action from a subspace for a discrete linear stochastic dynamical system. *Comput. Methods Math. Phys.*, **46**, 1155–1167, doi:10.1134/S0965542506070062.
- Phipps, S. J., 2010: The CSIRO Mk3L climate system model v1.2. Antarctic Climate & Ecosystems CRC Tech. Rep. 4, 121 pp. [Available online at <http://www.acecrc.org.au/access/repository/resource/017d2618-bc4e-102e-bf5a-4040d04b55e4/Climate%20model%20manual.pdf>.]
- Ring, M. J., and R. A. Plumb, 2008: The response of a simplified GCM to axisymmetric forcings: Applicability of the fluctuation–dissipation theorem. *J. Atmos. Sci.*, **65**, 3880–3898, doi:10.1175/2008JAS2773.1.
- Risken, H., 1984: *The Fokker-Planck Equation: Methods of Solution and Applications*. Springer-Verlag, 444 pp.
- Santoso, A., M. H. England, and W. Cai, 2012: Impact of Indo-Pacific feedback interactions on ENSO dynamics diagnosed using ensemble climate simulations. *J. Climate*, **25**, 7743–7763, doi:10.1175/JCLI-D-11-00287.1.